

Mid-infrared surface-emitting photonic crystal microcavity light emitter on silicon

Binbin Weng,^{1,a)} Jiangang Ma,¹ Lai Wei,² Jian Xu,² Gang Bi,³ and Zhisheng Shi¹

¹*School of Electrical and Computer Engineering, University of Oklahoma, Norman, Oklahoma 73019, USA*

²*Department of Engineering Science and Mechanics, Pennsylvania State University, University Park, Pennsylvania 16802, USA*

³*School of Information and Electrical Engineering, Zhejiang University, Hangzhou, Zhejiang 310015, People's Republic of China*

(Received 14 October 2010; accepted 13 November 2010; published online 6 December 2010)

We describe an IV-VI semiconductor light emitter consisting of a PbSe/PbSrSe multiple quantum well active region grown by molecular beam epitaxy on a patterned Si(111) substrate with a two dimensional (2D) photonic crystal (PC) array. The 2D PC array was designed to form photonic band gaps around 1960 and 2300 cm^{-1} . Under pulsed optical pumping, light emission was observed with strongly coupled PC defect modes, which correspond well with simulated photonic band gaps. The observed spectral linewidth was around 10 cm^{-1} and the highest quantum efficiency measured was 12.8%. © 2010 American Institute of Physics. [doi:10.1063/1.3524239]

With the advantages of high quality (Q) factor and small mode volumes, two dimensional (2D) photonic crystal (PC) technique has drawn intensive interest in design and fabrication of light emitters that operate in the infrared (IR) region in the last decade.¹⁻³ The surface emission, circular beam, single mode, and low threshold operation of PC microcavity light emitters make them ideal for mid-IR gas analysis applications.⁴ However, with the impact of surface recombination after PC pattern etching, most IR PC microcavity based light emitters reported are only in the near-IR region with III-V InGaAsP material system, mainly due to its low nonradiative surface recombination rate.^{1,5} Although mid-IR photonic crystal distributed feedback (PCDFB) lasers that uses PC structure have been reported,^{6,7} such lasers operate on different principles compared with PC microcavity technique, and therefore they do not have the same advantages as PC microcavity light emitters.

In this letter, we report a PbSe/Pb_{0.97}Sr_{0.03}Se multiple quantum wells (MQWs) mid-IR PC microcavity light emitter. The MQW epitaxial structure was grown on Si substrate with patterned PC structure. This process avoided etching of epitaxial films and, therefore, alleviated the problem of surface recombination. Pulsed emission spectra demonstrated strong coupled PC defect modes with narrow linewidths. Such a PC light emitter in the mid-IR region has not been realized yet.

A commercial software package (OPTIFDTD) was used to design the PC structure and analyze its in-plane photonic band structure by plane-wave expansion method. The design parameters include the refractive index n of the epitaxial layer, the interhole spacing a , and the radius of the air holes R . Refractive indices for PbSe and Pb_{0.97}Sr_{0.03}Se were reported previously.⁸ For PbSe/Pb_{0.97}Sr_{0.03}Se MQW structure, a weighted average value was used. Previously, we have reported a theoretical simulation with submicron scale design, which demonstrated a high Q factor TM band structure with a first order energy gap (3.959~5.872 μm) in the mid-IR region.⁹ For our proof-of-concept experimental demonstra-

tion in this letter, we intentionally increased the values of interhole spacing and radius of the air holes to micrometer range in order to allow high tolerance for possible errors in etching and lateral growth. Consequently, the first order photonic band gap is shifted to the far-IR spectral region, and higher order (second and third) energy gaps move into the mid-IR spectral region of interest. The calculated band diagram with $a=2.75 \mu\text{m}$ and $R=1.15 \mu\text{m}$ is shown in Fig. 1. The inset displays the first Brillouin zone in reciprocal space. Defect modes will be created in each photonic band gap by removing a single hole in the center of PC patterns. Based on the temperature dependent gain spectra of PbSe/Pb_{0.97}Sr_{0.03}Se MQW, we expect to observe two PC defect modes around the second and third order PC energy gaps of 1960 and 2300 cm^{-1} .

Experimentally, the central area of a $1 \times 1 \text{ cm}^2$ Si(111) substrate was patterned by a $1 \times 1 \text{ mm}^2$ hexagonal PC hole-array using electron-beam lithography. Defect modes were created by removing a single hole to form a microcavity in the middle of the PC pattern. There are 7×7 PC microcavi-

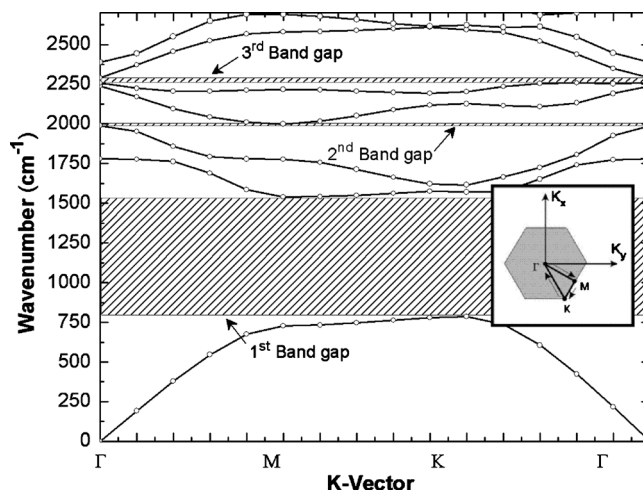


FIG. 1. Dispersion diagram of 2D TM modes of the hexagonal photonic crystal holes array; the first Brillouin zone in reciprocal space is displayed in the inset.

^{a)}Electronic mail: binbinweng@ou.edu.

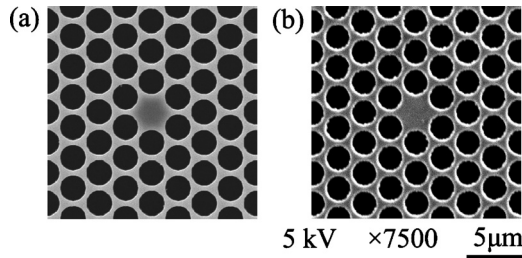


FIG. 2. Top view SEM image of (a) patterned Si(111) substrate; (b) PbSe/PbSrSe MQW structure grown on patterned Si(111).

ties in the patterned area in order to ensure enough power output. Patterned substrate was then dry-etched by a deep reactive ion etching (RIE) system to produce the pattern with etching depth of $3\mu\text{m}$. Figure 2(a) shows top view image of one PC microcavity patterned area of Si(111) substrate after RIE.

A custom-designed two-chamber MBE system was used for the growth, and a modified Shiraki cleaning method was used to clean the Si substrate before MBE growth. A CaF_2 layer of 2 nm that is within the critical thickness was grown on patterned Si(111) as a buffer layer in one chamber. IV-VI epitaxial structure was then grown on CaF_2/Si substrates in another chamber without breaking the vacuum. The epitaxial structure consisted of a seven-pair PbSe/ $\text{Pb}_{0.97}\text{Sr}_{0.03}\text{Se}$ MQW with 17 nm thick PbSe wells sandwiched between 25 nm thick $\text{Pb}_{0.97}\text{Sr}_{0.03}\text{Se}$ barrier layers. An $1\mu\text{m}$ BaF_2 layer was grown on top of MQW structure for vertical optical-confinement. Figure 2(b) shows a top view SEM image after epitaxial growth on patterned Si(111) substrate shown in Fig. 2(a).

After growth, the sample was directly mounted onto a copper holder without any further processing, and then placed into a LN_2 -cooled cryostat. The emission spectra were characterized by a Fourier transform infrared (FTIR) spectrometer (Bruker IFS 66/S) in step-scan mode with a $1.064\mu\text{m}$ Q-switched Nd:YAG (Surelight) pumping laser ($\tau_{\text{pulse}}=5\text{ ns}, 10\text{ Hz}$). Measurements on the sample were taken at both inside and outside the PC patterned area. The spot size of pumping laser is $\sim 1.5\text{ mm}$, which can cover the entire PC patterned area on the sample. Radiation of emission was then collected by a reflective objective made up of two off-axis parabolic mirrors and two planar mirrors. After that, the signal went through the FTIR spectrometer system with a $2.5\mu\text{m}$ long-wavelength-pass filter that cut off the signal of pumping laser and was detected by a LN_2 -cooled HgCdTe (MCT) detector.

Figure 3(a) displays the temperature dependent photoluminescence (PL) spectra of the unpatterned planar area on the sample. As temperature increases the emission peak shifts to higher energy. This agrees well with the temperature dependent IV-VI semiconductor QW gain spectra. The light emission spectra for the epitaxial layer grown on PC patterned Si are shown in Fig. 3(b). These spectra demonstrate two temperature-independent defect-mode peaks at around 1960 and 2300 cm^{-1} , which agree well with the calculated photonic band structure in Fig. 1. There is only one defect mode that appears in each spectrum at a given temperature. The second order PC defect mode at 1960 cm^{-1} dominates for $77\sim 160\text{ K}$ and the third order defect mode at 2300 cm^{-1} dominates for $180\sim 270\text{ K}$. This phenomenon is

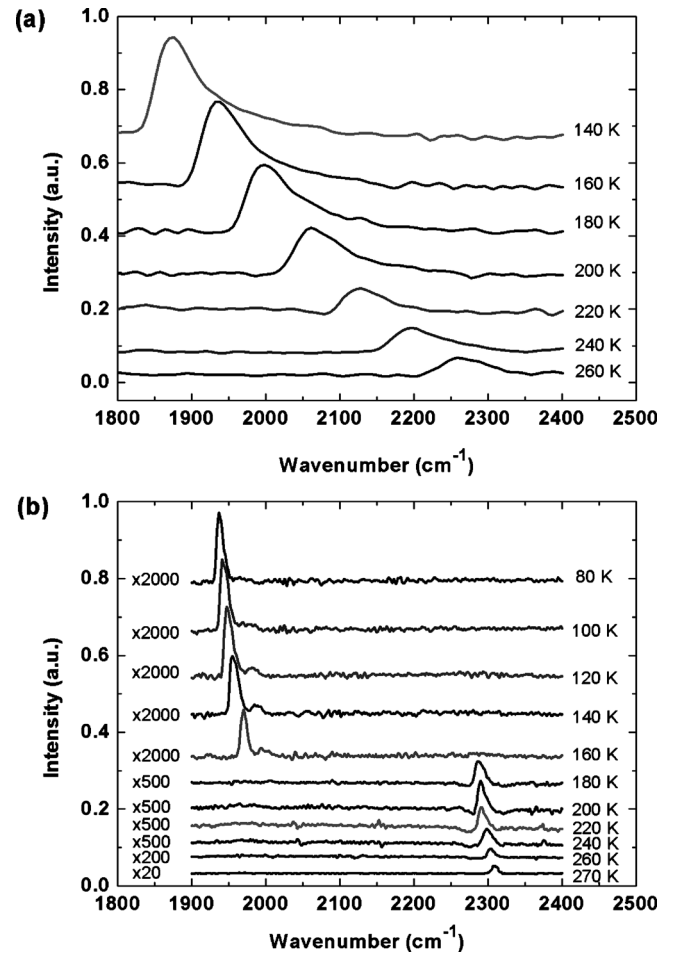


FIG. 3. Temperature-dependent PL emission of (a) PbSe/PbSrSe MQW on unpatterned Si(111); (b) PbSe/PbSrSe MQW on patterned Si(111).

due to the shift of the PbSe/PbSrSe MQW gain spectra to higher energy with the temperature. The measured linewidths of the PC defect modes are all about 10 cm^{-1} , which is much narrower than that of the normal spontaneous emission in PbSe/PbSrSe MQW structure. The weak blueshifts in both modes are caused by the refractive index variation with the temperature changes.⁸

Output emission power was calibrated by a standard blackbody reference source (Infrared Systems Development Corporation IR-580/301). Figure 4 shows collected output powers of both spontaneous and PC defect modes under the same average pumping laser power of 0.05 mW (1 kW peak pumping power). As can be seen from Fig. 4, the collected output power from PC defect modes is over two orders of magnitudes higher than that of PL emission. There are several factors for such significant enhancement of PC defect mode emission compared with spontaneous emission. First of all, the PC microcavity forces all the photons generated inside the cavity to funnel through its given modes and be extracted, whereas the extraction efficiency of PL emission from the planar epilayer is low under the total reflection limitation. Second, the narrow beam divergence of the emission from the PC structure increases the collecting efficiency. Third, great improvement in material quality due to the growth on patterned substrate could significantly reduce the material losses.¹⁰

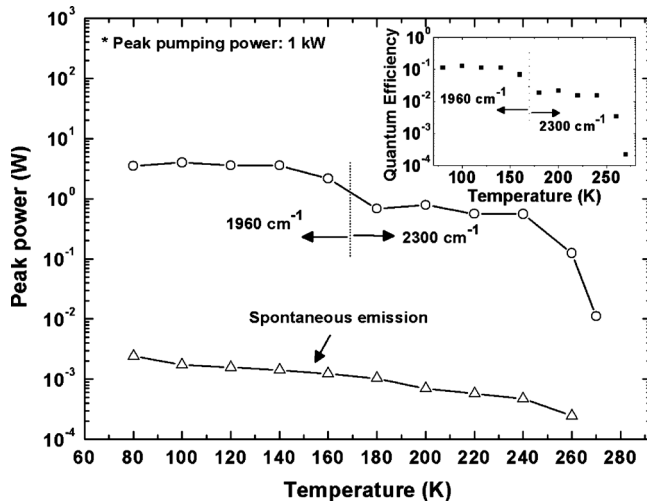


FIG. 4. Calibrated temperature dependent output emission power from PC microcavity and PbSe/PbSrSe MQW structure on unpatterned area. Quantum efficiency of the PC emission is shown in the inset.

Furthermore, the quantum efficiency (η_{quantum}) is calculated by the measured overall efficiency (η_{overall}) expressed as

$$\eta_{\text{overall}} = \eta_{\text{quantum}} \cdot \eta_{\text{pumping}} \cdot \eta_{\text{coupling}},$$

in which η_{pumping} and η_{coupling} are pumping efficiency and coupling efficiency, respectively. η_{pumping} is the ratio of the energy band gap of the quantum well at a certain temperature and pumping laser energy, assuming one pumping photon generates one electron-hole pair. The coupling efficiency consists of the reflective losses of the pumping laser on

IV-VI film and the effective pumping area. As shown in the inset of Fig. 4, the highest measured quantum efficiency of 12.8% appears at 100 K.

In conclusion, we have demonstrated a IV-VI midinfrared surface-emitting PC microcavity light emitter with strongly coupled defect mode emission. The highest peak output power and quantum efficiency measured are 3.99 W and 12.8%, respectively. The linewidths of those defect modes emission observed are only 10 cm^{-1} . With further optimization of design and growth parameters, we anticipate to make further progress in future.

Funding was partially provided by the DoD ARO under Grant No. W911NF-07-1-0587, STTR program of Missile Defense Agency under Contract No. HQ0006-07-C-7657, NSF Grant No. DMR-0520550, and by Oklahoma OCAST program under Grant No. AR082-052.

- ¹O. Painter, R. K. Lee, A. Scherer, A. Yariv, J. D. O'Brien, P. D. Dapkus, and I. Kim, *Science* **284**, 1819 (1999).
- ²M. Lončar, T. Yoshie, A. Scherer, P. Gogna, and Y. Qiu, *Appl. Phys. Lett.* **81**, 2680 (2002).
- ³Y. Akahane, T. Asano, B. S. Song, and S. Noda, *Nature (London)* **425**, 944 (2003).
- ⁴M. Tacke, *Infrared Phys. Technol.* **36**, 447 (1995).
- ⁵T. Baba and T. Matsuzaki, *Jpn. J. Appl. Phys., Part 1* **35**, 1348 (1996).
- ⁶I. Vurgaftman and J. R. Meyer, *Appl. Phys. Lett.* **78**, 1475 (2001).
- ⁷M. Kim, C. S. Kim, W. W. Bewley, J. R. Lindle, C. L. Canedy, I. Vurgaftman, and J. R. Meyer, *Appl. Phys. Lett.* **88**, 191105 (2006).
- ⁸A. Majumdar, H. Z. Xu, F. Zhao, J. C. Keay, L. Jayasinghe, S. Khosravani, X. Lu, V. Kelkar, and Z. Shi, *J. Appl. Phys.* **95**, 939 (2004).
- ⁹S. Mukherjee, G. Bi, J. P. Kar, and Z. Shi, *Opt. Appl.* **39**, 499 (2009).
- ¹⁰B. Weng, F. Zhao, J. Ma, G. Yu, J. Xu, and Z. Shi, *Appl. Phys. Lett.* **96**, 251911 (2010).